



# Fast tunneling Jahn–Teller isomer of the $[\text{Mn}_{12}\text{O}_{12}(\text{O}_2\text{CC}_6\text{H}_4\text{-2-CH}_3)_{16}(\text{H}_2\text{O})_4] \cdot \text{S}$ single-molecule magnet

Evan M. Rumberger<sup>a</sup>, Enrique del Barco<sup>c</sup>, Jon Lawrence<sup>b</sup>, Stephen Hill<sup>b</sup>,  
Andrew D. Kent<sup>c</sup>, Lev N. Zakharov<sup>a</sup>, Arnold L. Rheingold<sup>a</sup>, David N. Hendrickson<sup>a,\*</sup>

<sup>a</sup> Department of Chemistry and Biochemistry – 0358, University of California at San Diego, La Jolla, CA 92093-0358, United States

<sup>b</sup> Department of Physics, University of Florida, Gainesville, FL 32611, United States

<sup>c</sup> Department of Physics, New York University, New York, NY 10003, United States

Received 5 October 2004; accepted 28 December 2004

Available online 11 July 2005

## Abstract

The single-crystal X-ray structure of the single-molecule magnet  $[\text{Mn}_{12}\text{O}_{12}(\text{O}_2\text{CC}_6\text{H}_4\text{-2-CH}_3)_{16}(\text{H}_2\text{O})_4] \cdot \text{CH}_2\text{Cl}_2 \cdot 2\text{H}_2\text{O}$  (complex **1**) is reported. Complex **1** is a new example of a “Jahn–Teller isomer”, since it has two Mn(III) ions with abnormally oriented Jahn–Teller elongation axes. Complex **1** has a lower activation energy ( $U_{\text{eff}} = 29$  K) for magnetization reversal relative to other reported  $[\text{Mn}_{12}\text{O}_{12}]$  type molecules (e.g.,  $U_{\text{eff}} = 70$  K for  $\text{Mn}_{12}\text{Ac}$ ). Single-crystal low temperature magnetization measurements are reported that confirm that complex **1** is a single-molecule magnet. High-field electron paramagnetic resonance measurements were performed on a single crystal to give the spin Hamiltonian parameters.

© 2005 Elsevier Ltd. All rights reserved.

**Keywords:** Single-molecule magnet; Quantum tunneling of magnetization; Nanomagnet; Superparamagnet

## 1. Introduction

The most thoroughly studied single-molecule magnet (SMM)  $[\text{Mn}_{12}\text{O}_{12}(\text{O}_2\text{CCH}_3)_{16}(\text{H}_2\text{O})_4]$ , or  $\text{Mn}_{12}\text{Ac}$  for short, has served as an excellent starting material for the synthesis of an assortment of new SMMs [3–13]. A large variety of these molecules, each possessing the  $[\text{Mn}_{12}\text{O}_{12}]$  core, have been synthesized by taking advantage of the facile carboxylate ligand substitution that  $\text{Mn}_{12}\text{Ac}$  undergoes. Many of these ligand substitution products have very different magnetic properties when compared to  $\text{Mn}_{12}\text{Ac}$ . The most striking difference is often observed in the out-of-phase component of the variable-temperature ac magnetic susceptibility plots.

Bulk polycrystalline samples frequently exhibit *two* out-of-phase peaks in their ac susceptibility versus temperature plots [14,15]. These two different ac responses often occur in two distinct temperature regimes for a given applied ac field; one peak is observed within the 5–10 K range, while the other is observed in the 2–4 K range. These two different responses have been coined as high-temperature (HT) and low-temperature (LT) peaks, respectively. The presence of two different responses in the ac out-of-phase magnetic susceptibility implies that there are at least two different magnetization relaxation mechanisms. Understanding the origins of these two different responses has been the subject of several recent studies [16–25]. It has been found that the structural origins of these two different magnetization relaxation mechanisms originate from different isomers of the  $[\text{Mn}_{12}\text{O}_{12}]$  molecule [16,17,20–23]. Careful control of synthetic and crystallization conditions can

\* Corresponding author.

E-mail address: [dhendrickson@ucsd.edu](mailto:dhendrickson@ucsd.edu) (D.N. Hendrickson).

yield chemically pure crystals of either the HT or LT forms. In some cases, ac susceptibility measurements show that a single-crystal can either have a HT or LT peak, but *not* both. The majority of crystal structures reported for  $[\text{Mn}_{12}\text{O}_{12}(\text{O}_2\text{CR})_{16}(\text{H}_2\text{O})_4]$  complexes exhibit HT behavior and have activation energies towards magnetization reversal of  $U_{\text{eff}} = 60\text{--}70$  K. A much smaller family of  $[\text{Mn}_{12}\text{O}_{12}(\text{O}_2\text{CR})_{16}(\text{H}_2\text{O})_4]$  are LT and have activation energies in the 20–40 K range. Crystal structures of each isomer can be solved. The LT form has an abnormally oriented Jahn–Teller axis in the coordination geometry of one or more of the  $\text{Mn}^{\text{III}}$  ions. These abnormal Jahn–Teller axes are oriented towards a  $\mu_3$ -oxide which, topographically, reside near the plane of the disc-like shape of the  $[\text{Mn}_{12}\text{O}_{12}]$  core. The HT form does not have an abnormally oriented Jahn–Teller axis at a  $\text{Mn}^{\text{III}}$  ion. This phenomenon has been coined “Jahn–Teller isomerism” (JTI). In this paper, we report the characterization of a new LT complex,  $[\text{Mn}_{12}\text{O}_{12}(\text{O}_2\text{CC}_6\text{H}_4\text{-2-CH}_3)_{16}(\text{H}_2\text{O})_4] \cdot \text{S}$ .

## 2. Experimental

### 2.1. Synthesis

All solvents and reagents were used as received. All reactions were performed under aerobic conditions.

$[\text{Mn}_{12}\text{O}_{12}(\text{O}_2\text{CC}_6\text{H}_4\text{-2-CH}_3)_{16}(\text{H}_2\text{O})_4] \cdot \text{CH}_2\text{Cl}_2 \cdot 2\text{H}_2\text{O}$  (complex **1**). Multiple treatments of a toluene slurry of  $\text{Mn}_{12}\text{Ac}$  (4.0 g, 1.94 mmol) with a large excess of 2-methylbenzoic acid (8.7 g, 63.9 mmol) followed by solvent removal and washing of the excess carboxylate ligand with ethanol yields the product  $[\text{Mn}_{12}\text{O}_{12}(\text{O}_2\text{CC}_6\text{H}_4\text{-2-CH}_3)_{16}(\text{H}_2\text{O})_4]$ . *Anal. calc.* for  $\text{C}_{128}\text{H}_{120}\text{Mn}_{12}\text{O}_{48}$ : C, 49.8; H, 3.9. *Found*: C, 50.3; H, 3.8%. Crystallization solvents were saturated with 2-methylbenzoic acid before their use. Crystallization is achieved by layering a  $\text{CH}_2\text{Cl}_2$  solution of complex **1** with hexanes. Over a period of three weeks, block shaped crystals with the formula  $[\text{Mn}_{12}\text{O}_{12}(\text{O}_2\text{CC}_6\text{H}_4\text{-2-CH}_3)_{16}(\text{H}_2\text{O})_4] \cdot 2\text{H}_2\text{O} \cdot \text{CH}_2\text{Cl}_2$  precipitate from the solution.

### 2.2. Physical measurements

High frequency electron paramagnetic resonance (HFEP) measurements were performed on home made instrumentation described elsewhere [26]. Low temperature magnetization versus field data were collected using a micro-Hall effect magnetometer which is described in [27]. Practical considerations of the crystal morphology for complex **1** meant that the magnetic field orientation for the data presented in both the single-crystal HFEP and single-crystal magnetization studies was  $\sim 45^\circ$  away from the easy axis of **1**.

## 3. Results and discussion

### 3.1. Description of structure

Several relevant crystal structure parameters are listed in Table 1 for complex **1**. The crystal structure for  $[\text{Mn}_{12}\text{O}_{12}(\text{O}_2\text{CC}_6\text{H}_4\text{-2-CH}_3)_{16}(\text{H}_2\text{O})_4] \cdot \text{CH}_2\text{Cl}_2 \cdot 2\text{H}_2\text{O}$  (**1**) is illustrated in Fig. 1. Complex **1** crystallizes in the monoclinic  $C2/c$  space group. The atoms Mn(5) and Mn(5a), which are related by a crystallographic C2 axis, have an unusually oriented Jahn–Teller axis. This abnormally oriented Jahn–Teller axis contains an oxide ion, O(1), a situation which is highly unusual: JT elongation axes usually orient so as to avoid the strong  $\text{Mn(III)-O}^{2-}$  bonds, normally the shortest bonds about a Mn(III) ion. These abnormally oriented Jahn–Teller axes reside nearly in the plane of the ring formed by the eight Mn(III) surrounding the cubane core. The other six Mn(III) ions have their Jahn–Teller elongation axis situated essentially parallel to each other and orthogonal to the plane of the ring of Mn(III) ions.

### 3.2. Alternating current magnetic susceptibility studies

Ac magnetic susceptibility data were collected for a single-crystal sample of complex **1** in the 1.8–10 K range with a 3 Oe ac field oscillating in the frequency range of 50–1000 Hz. The external dc magnetic field was fixed at zero. Complex **1** is a LT form and exhibits an out-of-phase peak in its ac susceptibility in the 2–4 K region as seen in Fig. 2. The appearance of frequency dependent peaks in the out-of-phase ac susceptibility is evidence for slow magnetization relaxation dynamics relative to the frequency of the applied oscillating ac field. The magnetization relaxation rates can be

Table 1  
Crystallographic parameters for complex **1**

Complex	<b>1</b>
Solvate (S)	$\text{CH}_2\text{Cl}_2 \cdot 2\text{H}_2\text{O}$
Crystal system	monoclinic
Space group	$C2/c$
Crystal habit	block
$a$ (Å)	17.4305(9)
$b$ (Å)	38.214(2)
$c$ (Å)	21.0129(11)
$\alpha$ (°)	90
$\beta$ (°)	98.5610(10)
$\gamma$ (°)	90
$V$ (Å <sup>3</sup> )	13840.6(12)
$Z$	4
Temperature (K)	100(2)
Reflections collected	43 649
Number of observed reflections	13 003
Independent reflections	15 785
Final $R$ indices [ $I > 2\sigma(I)$ ]	$R_1 = 0.0837$
$R$ indices (all data)	$R_1 = 0.0960$
Goodness-of-fit on $F^2$	0.870

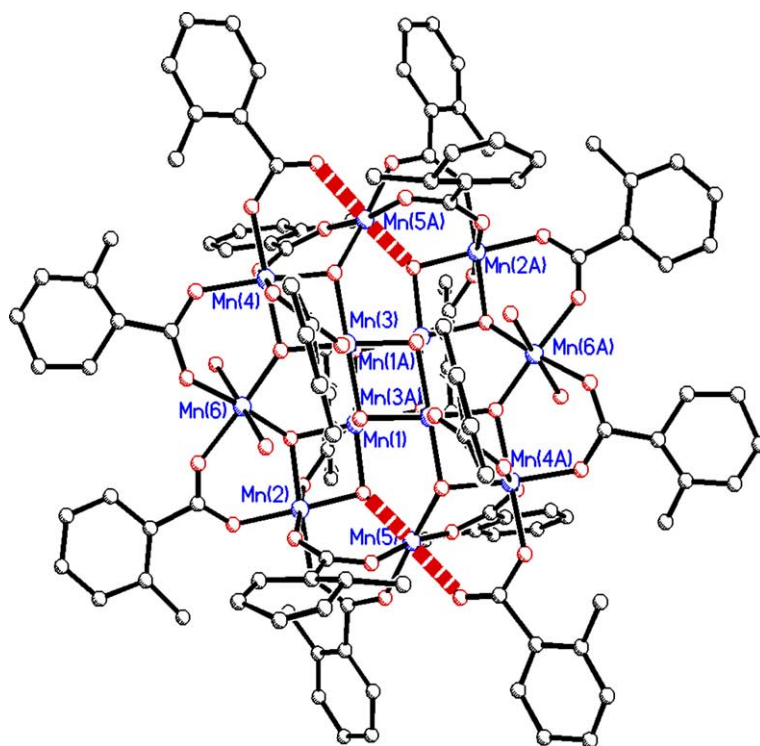


Fig. 1. ORTEP representation of the LT complex  $[\text{Mn}_{12}\text{O}_{12}(\text{O}_2\text{CC}_6\text{H}_4\text{-}2\text{-CH}_3)_{16}(\text{H}_2\text{O})_4] \cdot \text{CH}_2\text{Cl}_2 \cdot 2\text{H}_2\text{O}$  (complex 1). The thick dashed lines represent abnormally oriented Jahn–Teller axes.

quantified by analyzing the frequency dependencies of the  $\chi''_{\text{M}}$  signals for the two complexes as shown in Fig. 2. Data were collected for several ac frequencies in the 50–1000 Hz range and the maxima of the  $\chi''_{\text{M}}$  were used in conjunction with the Arrhenius equation

$$\ln(1/\tau) = \ln(1/\tau_0) - U_{\text{eff}}/kT \quad (1)$$

to calculate the barrier towards magnetization reversal as  $U_{\text{eff}} = 29$  K for complex 1. Complex 1 has an activation energy towards magnetization reversal,  $U_{\text{eff}}$ , that is

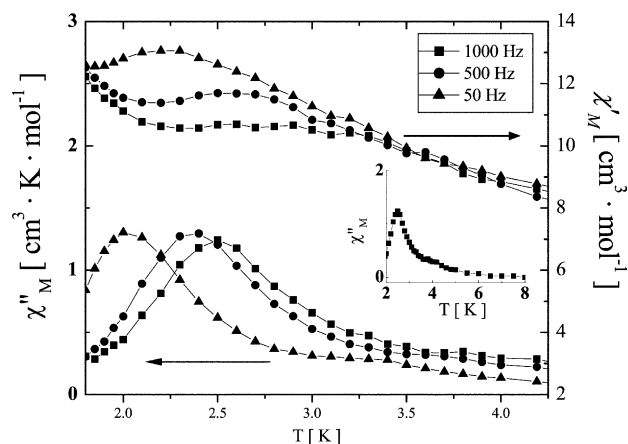


Fig. 2. Plot of the variable-temperature ac susceptibility for a single crystal of complex (1) collected for several frequencies. The in-phase responses are shown in the upper part of the plot, whereas the out-of-phase responses are shown in the lower part.

nearly half of its parent compound,  $\text{Mn}_{12}\text{Ac}$ , which has an activation energy of  $U_{\text{eff}} = 62$  K.

### 3.3. Magnetization versus magnetic field hysteresis

Fig. 3 shows the single-crystal magnetization hysteresis data for complex 1 measured at 0.38 K for two

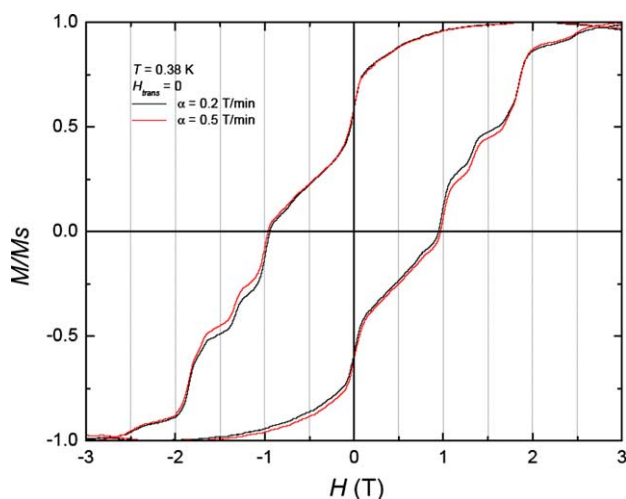


Fig. 3. Plot of the normalized magnetization ( $M/M_S$ ) vs. magnetic field ( $H$ ), where  $M_S$  is the saturation magnetization. Data were collected on a single crystal at a temperature of 0.38 K and scanning rates of 0.2 and 0.5 T/min with the longitudinal magnetic field  $\sim 45^\circ$  away from the easy axis.

different sweep rates, 0.2 and 0.5 T/min. The applied magnetic field was  $\sim 45^\circ$  away from the easy axis of magnetization. A complex hysteresis loop is observed. The observation of an appreciable coercive field along with magnetic field sweep rate dependent steps in the hysteresis loop for the field interval between 1 and 3 T confirms the single-molecule magnet behavior of **1**. The steps are due to quantum tunneling of the magnetization. There is also a large step observed at zero magnetic field.

### 3.4. High frequency EPR (HFEP) studies

In order to determine the ground state spin Hamiltonian parameters for complex **1**, HFEP) data of a single-

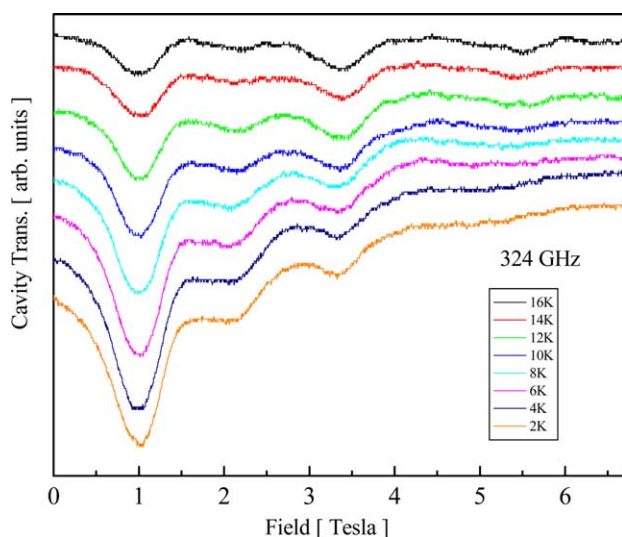


Fig. 4. HFEP) spectra measured at 324 GHz for a single-crystal sample of complex **1**. Data were collected at the temperatures of 2, 4, 6, 10, 12, 14, and 16 K with the magnetic field oriented  $\sim 40^\circ$  to the easy axis direction.

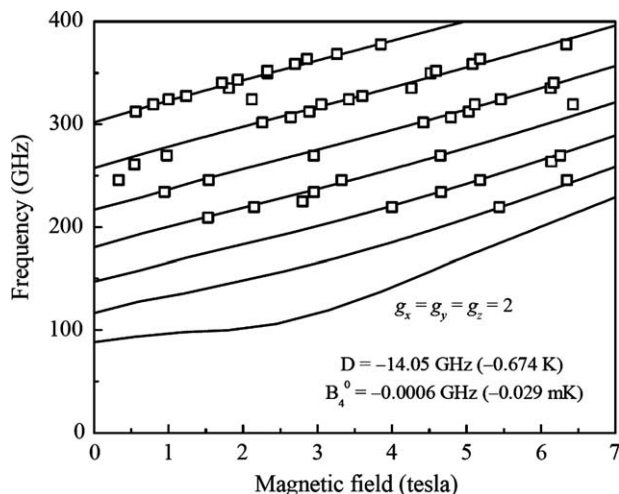


Fig. 5. Zeeman diagram for the spin Hamiltonian associated with the  $S = 10$  ground state of complex **1** with the magnetic field oriented  $\sim 40^\circ$  to the easy axis direction. The solid lines represent the energy spectrum obtained from the simulation to the resonances.

crystal sample were collected. The spectra are shown in Fig. 4 for a microwave frequency of 324 GHz and at temperatures of 2, 4, 6, 8, 10, 12, 14, and 16 K. The frequency dependence of several resonances were simulated using an  $S = 10$  spin Hamiltonian. The Zeeman interaction, axial zero-field splitting,  $D(\hat{S}_z^2)$ , and the fourth order zero-field term,  $B_4^0 \hat{O}_4^0$ , were included in the analysis. Fig. 5 depicts the results obtained from the simulations of the resonances, which are consistent with the following parameters:  $g_z = g_x = g_y = 2.0$ ,  $D = -0.47 \text{ cm}^{-1}$ , and  $B_4^0 = -2.0 \times 10^{-5} \text{ cm}^{-1}$ .

## 4. Conclusion

The synthesis and crystal structure of a LT  $\text{Mn}_{12}$  complex are reported. Steps, with the most pronounced having field intervals of  $\sim 0.8$  T, are observed in magnetization hysteresis plots collected for a single crystal at millikelvin temperatures. These steps confirm that **1** behaves as a single-molecule magnet. HFEP) data collected on this sample allowed for the quantitative characterization of the spin Hamiltonian parameters  $g_z = g_x = g_y = 2.0$ ,  $D = -0.47 \text{ cm}^{-1}$ , and  $B_4^0 = -2.0 \times 10^{-5} \text{ cm}^{-1}$ . The resonance positions of the steps seen in the magnetization hysteresis plot are consistent with the parameters obtained from the EPR studies when the  $\sim 45^\circ$  angle between the easy axis and magnetic field is taken into consideration ( $0.8\cos(45^\circ) \approx 0.5$ ).

## Acknowledgments

This work was supported by the National Science Foundation (CHE0350615, DMR0103290 and DMR0239481). S.H. is a Cottrell scholar of the Research Corporation.

## References

- [1] G. Christou, D. Gatteschi, D.N. Hendrickson, R. Sessoli, MRS Bull. 25 (11) (2000) 66.
- [2] D. Gatteschi, R. Sessoli, Angew. Chem. Int. Ed. 42 (3) (2003) 268.
- [3] R. Sessoli, H.L. Tsai, A.R. Schake, S.Y. Wang, J.B. Vincent, K. Folting, D. Gatteschi, G. Christou, D.N. Hendrickson, J. Am. Chem. Soc. 115 (5) (1993) 1804.
- [4] D. Ruiz-Molina, G. Christou, D.N. Hendrickson, Mol. Cryst. Liq. Cryst. 343 (2000) 335.
- [5] M. Soler, S.K. Chandra, D. Ruiz, J.C. Huffman, D.N. Hendrickson, G. Christou, Polyhedron 20 (11–14) (2001) 1279.
- [6] M. Soler, S.K. Chandra, D. Ruiz, E.R. Davidson, D.N. Hendrickson, G. Christou, Chem. Commun. (24) (2000) 2417.
- [7] P. Gerbier, D. Ruiz-Molina, N. Domingo, D.B. Amabilino, J. Vidal-Gancedo, J. Tejada, D.N. Hendrickson, J. Veciana, Monatsh Chem. 134 (2) (2003) 265.
- [8] T. Kuroda-Sowa, M. Lam, A.L. Rheingold, C. Frommen, W.M. Reiff, M. Nakano, J. Yoo, A.L. Maniero, L.C. Brunel, G. Christou, D.N. Hendrickson, Inorg. Chem. 40 (25) (2001) 6469.

- [9] A.R. Schake, H.L. Tsai, N. Devries, R.J. Webb, K. Folting, D.N. Hendrickson, G. Christou, *J. Chem. Soc., Chem. Commun.* 5 (2) (1992) 181.
- [10] A.R. Schake, H.L. Tsai, R.J. Webb, K. Folting, G. Christou, D.N. Hendrickson, *Inorg. Chem.* 33 (26) (1994) 6020.
- [11] H.L. Tsai, T.Y. Jwo, G.H. Lee, Y. Wang, *Chem. Lett.* (4) (2000) 346.
- [12] H.L. Tsai, D.M. Chen, C.I. Yang, T.Y. Jwo, C.S. Wur, G.H. Lee, Y. Wang, *Inorg. Chem. Commun.* 4 (9) (2001) 511.
- [13] G. Aromi, S.M.J. Aubin, M.A. Bolcar, G. Christou, H.J. Eppley, K. Folting, D.N. Hendrickson, J.C. Huffman, R.C. Squire, H.L. Tsai, S. Wang, M.W. Wemple, *Polyhedron* 17 (17) (1998) 3005.
- [14] H.J. Eppley, S.M.J. Aubin, M.W. Wemple, D.M. Adams, H.L. Tsai, V.A. Grillo, S.L. Castro, Z.M. Sun, K. Folting, J.C. Huffman, D.N. Hendrickson, G. Christou, *Mol. Cryst. Liq. Cryst. A* 305 (1997) 167.
- [15] D. Ruiz, Z.M. Sun, B. Albela, K. Folting, J. Ribas, G. Christou, D.N. Hendrickson, *Angew. Chem., Int. Ed. Engl.* 37 (3) (1998) 300.
- [16] S.M.J. Aubin, Z. Sun, E.M. Rumberger, D.N. Hendrickson, G. Christou, *J. Appl. Phys.* 91 (10) (2002) 7158.
- [17] S.M.J. Aubin, Z.M. Sun, H.J. Eppley, R.M. Rumberger, I.A. Guzei, K. Folting, P.K. Gantzel, A.L. Rheingold, G. Christou, D.N. Hendrickson, *Polyhedron* 20 (11–14) (2001) 1139.
- [18] M. Soler, W. Wernsdorfer, Z.M. Sun, J.C. Huffman, D.N. Hendrickson, G. Christou, *Chem. Commun.* (21) (2003) 2672.
- [19] N. Soler, W. Wernsdorfer, Z.M. Sun, D. Ruiz, J.C. Huffman, D.N. Hendrickson, G. Christou, *Polyhedron* 22 (14–17) (2003) 1783.
- [20] S.M.J. Aubin, Z.M. Sun, H.J. Eppley, E.M. Rumberger, I.A. Guzei, K. Folting, P.K. Gantzel, A.L. Rheingold, G. Christou, D.N. Hendrickson, *Inorg. Chem.* 40 (9) (2001) 2127.
- [21] D. Ruiz, Z.M. Sun, S.M.J. Aubin, E. Rumberger, C. Incarvito, K. Folting, A.L. Rheingold, G. Christou, D.N. Hendrickson, *Mol. Cryst. Liq. Cryst. A* 334 (1999) 1125.
- [22] Z.M. Sun, D. Ruiz, N.R. Dilley, M. Soler, J. Ribas, K. Folting, M.B. Maple, G. Christou, D.N. Hendrickson, *Chem. Commun.* (19) (1999) 1973.
- [23] Z.M. Sun, D. Ruiz, E. Rumberger, C.D. Incarvito, K. Folting, A.L. Rheingold, G. Christou, D.N. Hendrickson, *Inorg. Chem.* 37 (19) (1998) 4758.
- [24] S.M.J. Aubin, Z.M. Sun, I.A. Guzei, A.L. Rheingold, G. Christou, D.N. Hendrickson, *Chem. Commun.* (22) (1997) 2239.
- [25] S.M.J. Aubin, Z.M. Sun, I.A. Guzei, A.L. Rheingold, G. Christou, D.N. Hendrickson, *Chem. Commun.* (22) (1997) 2239.
- [26] M. Mola, S. Hill, P. Goy, M. Gross, *Rev. Sci. Instrum.* 71 (1) (2000) 186.
- [27] A.D. Kent, S. von Molnar, S. Gider, D.D. Awschalom, *J. Appl. Phys.* 76 (10) (1994) 6656.